Molecular Flasks

DOI: 10.1002/ange.201004879

Switchable Open-Cage Fullerene for Water Encapsulation**

Qianyan Zhang, Tobias Pankewitz, Shuming Liu, Wim Klopper, and Liangbing Gan**

Fullerenes have a cavity large enough to encapsulate atoms and molecules.[1] Making a suitable hole in the fullerene cage followed by attaching an easily removable stopper into the orifice can produce a single-molecule-based vial. There are many possible applications for such a vial; for example, it may be used as a carrier for radioactive atoms or small molecules such as tritiated water (T_2O) in radiopharmaceuticals for diagnostic or therapeutic studies. Over the past decade, much progress has been made in the area of fullerene cage opening.[2] A number of open-cage fullerenes have been reported, some of which can encapsulate small organic molecules.[3] However, there have been no successful attempts to cover the orifice with a removable blocker. The known open-cage fullerenes are analogous to a round-bottom flask without a stopper. Herein, we report the preparation of the first open-cage fullerene with a stopper that can be attached and removed through a single-step reaction. Water was shown to be effectively trapped by the present compound.

We recently reported the preparation of compound **1a** and its water-encapsulated complex H_2O@**1a** through a peroxide-mediated cage-opening strategy.[4] Carbonyl groups on the rim of the orifice are quite reactive towards various nucleophiles. Treatment of **1** with triethylphosphite resulted in compound **2** with a phosphate group attached above the orifice (Scheme 1). Under basic conditions, the phosphate can be hydrolyzed to retrieve compound **1**. The phosphate formation reaction is more efficient than the hydrolysis process, as the reaction time at room temperature is 10 min for the forward reaction but 2 h for the backward hydrolysis reaction.

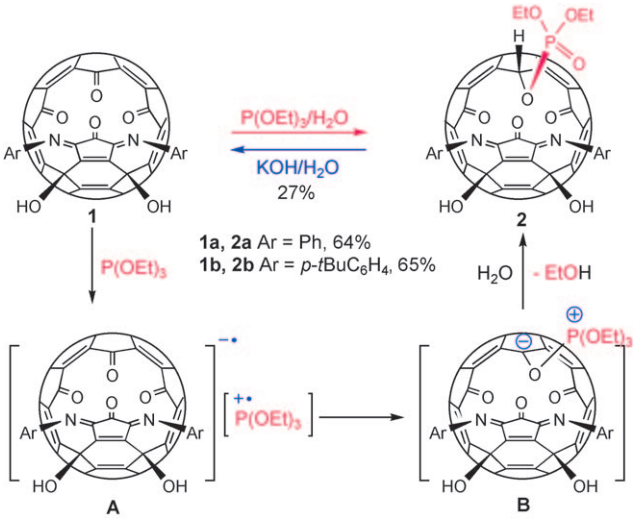

Scheme 1. Addition of a phosphate blocker to the orifice.

The formation of the phosphate moiety in compound **2** was unexpected. Analogous reactions of classical organic carbonyl compounds with triethylphosphite usually yield α-hydroxy phosphonates (Abramov reaction)[5] with the phosphorus atom connected to the carbonyl carbon atom, whereas the hydrogen atom is connected to the carbonyl oxygen atom. The opposite is observed in the present reaction with compound **1**. A possible mechanism is proposed in Scheme 1. Owing to the electron-deficient nature of the fullerene cage and the presence of carbonyl groups in compound **1**, single electron transfer is favored in the first step instead of phosphite attack at the carbonyl carbon atom. The so-formed radical ion pair **A** then forms the zwitterionic intermediate **B** through formation of an O–P bond. Steric hindrance is probably responsible for the regioselectivity. Finally, protonation of the carbon anion and hydrolysis of the phosphonium yields compound **2**. Alternatively, intermediate **B** may be formed through phosphorus attack at the carbonyl carbon atom to form a zwitterion, followed by a Phospha–Brook rearrangement.[6]

The structure of compound **2** was determined from spectroscopic data. The number of carbon signals in the ^{13}C NMR spectrum confirms the C_s symmetry of the structure. There is just one signal for the two hydroxy groups at $\delta = 7.63$ and 8.11 ppm for **2a** and **2b**, respectively, further supporting the C_s symmetry. The fullerenyl proton appears as a doublet at $\delta = 7.36$ (**2a**) and 7.6 ppm (**2b**) owing to coupling to the phosphorus atom. In the ^1H NMR spectrum of compound **2a**, there is a minor signal at $\delta = 7.64$ ppm and a minor doublet at $\delta = 7.37$ ppm, corresponding to the OH and fullerenyl proton groups for the water encapsulated compound H_2O@**2a**. Thus,

[*] Q. Y. Zhang, S. M. Liu, Prof. Dr. L. B. Gan
Beijing National Laboratory for Molecular Sciences, CAS Key Laboratory for Organic Solids, Institute of Chemistry, Chinese Academy of Science, Beijing 100080 (China)
Dr. T. Pankewitz, Prof. Dr. W. Klopper
Abteilung für Theoretische Chemie, Institut für Physikalische Chemie, Karlsruher Institut für Technologie, Postfach 6980, 76049 Karlsruhe (Germany)
Prof. Dr. W. Klopper
Center for Functional Nanostructures (CFN), Karlsruher Institut für Technologie, Postfach 6980, 76049 Karlsruhe (Germany)
E-mail: klopper@kit.edu
Prof. Dr. L. B. Gan
Key Laboratory of Bioorganic Chemistry and Molecular Engineering of the Ministry of Education, College of Chemistry and Molecular Engineering, Peking University, Beijing 100871 (China)
E-mail: gan@pku.edu.cn

[**] Financial support was provided by the NNSFC, MOST, and Deutsche Forschungsgemeinschaft (CFN subproject C3.3).
Supporting information for this article is available on the WWW under http://dx.doi.org/10.1002/anie.201004879.

just like in the case observed by Komatsu and co-workers,[7] proton chemical shifts on the rim of the orifice can be used to tell the difference in structure inside the cavity.

A single-crystal X-ray structure was obtained for H_2O@**2a** with near C_s symmetry (Figure 1). In agreement with the relatively low-field OH proton signal mentioned above, there

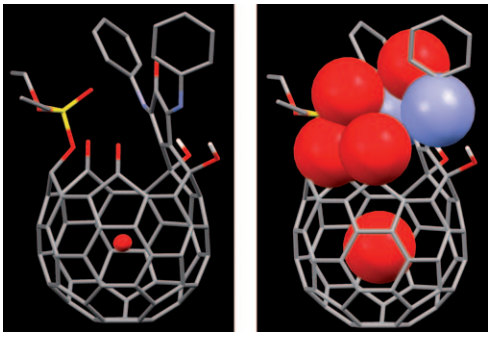

Figure 1. Single-crystal X-ray structure of H_2O@**2a**. Hydrogen atoms, except those of the OH groups, are omitted for clarity. Red O, yellow P, blue N, gray C, white H.

is strong intramolecular hydrogen bonding between the OH group and the adjacent imino nitrogen atom with O-H···N geometry of 2.16 Å (1.99 Å) and 134° (141°) for the two sets of almost equivalent hydrogen bonds. The phosphate moiety is clearly shown to be positioned above the orifice, whereas the fullerenyl hydrogen atom points away from the orifice. The two ethoxy groups are almost symmetrically located on the two sides of the mirror plane. A partial space-filling model (Figure 1 right) indicates that the orifice is significantly reduced and that it is quite difficult for the trapped water molecule to escape from the cage.

Experimental data support the above "stopper" effect of the phosphate moiety. A 1:1 mixture of empty compounds **1a** and **2a** was heated in C_6D_6 with excess water added at various temperatures (Figure 2). The process was monitored by ^{1}H NMR spectroscopy. The signal for the trapped water molecule in H_2O@**1a** was evident after 36 h at 60 °C. Continued heating of the same sample at 80 °C for 22 h increased the encapsulation ratio only of H_2O@**1a**, but the signal for H_2O@**2a** remained absent. A weak signal appeared for H_2O@**2a** only after heating the sample at 85 °C for another 22 h. In a related experiment, H_2O@**1a** (at about 80% encapsulation ratio) was heated in C_6D_6 with excess D_2O added. There was almost no change in the water signals for H_2O@**1a** at 45 °C for 24 h. When the temperature was increased to 60 °C, the signal for H_2O@**1a** began to decrease gradually. However, the same exchange experiment with H_2O@**2a** did not show any detectable signal decrease. These results indicate that the phosphate moiety in compound **2** serves as an efficient "stopper".

The encapsulation of a water molecule within the compounds **1a** and **2a** was studied by density functional theory including an empirical correction term for dispersion (DFT-D). In previous computational studies, this approach has provided reliable accuracy for chemically very similar sys-

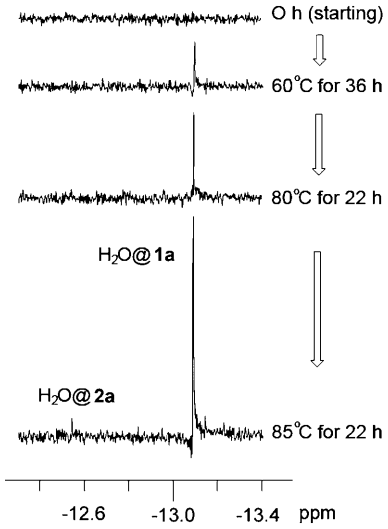

Figure 2. Water encapsulation for a mixture of **1a** and **2a** in C_6D_6/H_2O monitored by ^{1}H NMR spectroscopy.

tems, when benchmarking it to high-level wavefunction calculations.[8] In both equilibrium (EQ) structures H_2O@**1a** and H_2O@**2a**, the binding energy of the water molecule is −46 kJ mol^{-1}. The water molecule is located off-center, closer to the unaltered hemisphere of the cage and about 3.2 Å above the bottom pentagon in both open cages. In accordance with the X-ray structure, we found a strong intramolecular hydrogen bond bridging between the OH groups in the backbone of the cages and the imino groups (H_2O@**2a** (BP86-D/def2-TZVP): N···H 1.85 Å, O–H···N 143°). Apart from optimizing the equilibrium position of the water molecule within the cages, transition state (TS) searches for the water molecule leaving the cages were conducted (Figure 3). Because of the numerous degrees of freedom within the orifices, locating the TS is very demanding (for computational details refer to the Experimental Section). Within a small energy range of less than 5 kJ mol^{-1}, we found several stationary points only differing by the absolute position of the water molecule with respect to rotation around its axis. Thus, the displayed structures are expected to represent the TS structures rather closely.

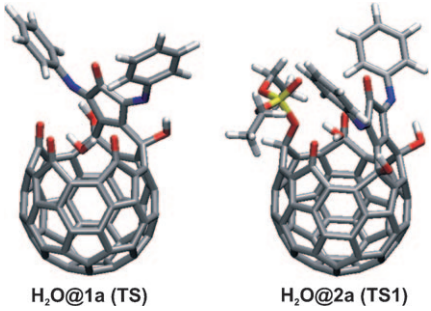

Figure 3. Adopted TS structures for the water molecule leaving the cage of **1a** and **2a**, respectively. The calculated barrier heights neglecting solvent effects are 106 kJ mol^{-1} for H_2O@**1a** and 129 kJ mol^{-1} for H_2O@**2a** (BP86-D/def2-TZVP//BP86-D/def2-SV(P)).

From Figure 3 it can be seen that in cage **2a** the maximum energy structure (the TS) for the water molecule leaving the cage is reached later than in **1a** with respect to the distance of the water molecule to the bottom pentagon of the cage (ca. 7.15 Å compared with ca. 6.5 Å, respectively). The calculated barrier heights (gas phase) are 106 kJ mol^{-1} in H_2O@**1a** and 129 kJ mol^{-1} in H_2O@**2a** (Table 1). Furthermore,

Table 1: Calculated energy barriers [kJ mol^{-1}] for the water molecule leaving (ΔE^{out}) and entering (ΔE^{in}) the cages (BP86-D/def2-TZVP//BP86-D/def2-SV(P)). Solvent effects on the barrier heights are estimated from the perpendicular scans with and without the COSMO model.

	H_2O@**1a**	H_2O@**2a**
ΔE^{in}	60	83
ΔE^{out}	106	129
ΔE^{in}(cosmo)	92	108
ΔE^{out}(cosmo)	106	122

H_2O@**2a** reveals a second, much lower barrier for the water molecule moving further out of the cage (the approximate TS2 structure lies about 53 kJ mol^{-1} below TS1), whereas there is only a single barrier present in H_2O@**1a**. For H_2O@**2a**, only the transition state associated with the higher of the two barriers (TS1) is shown in Figure 3 and is listed in Table 1, where also the barrier heights for the water molecule entering the cages from the outside are given. To interpret the dynamic ^{1}H NMR measurements performed in solution, the computed gas phase barriers were corrected for solvent effects employing a continuum solvation model. The corrections were estimated by comparing the potential curves of a perpendicular trajectory for the water moving towards the orifice in H_2O@**1a** and H_2O@**2a** calculated with and without the COSMO model (for details refer to the Experimental Section).

The solvent corrected energy barriers for the water molecule entering the cages of **1a** and **2a** (92 kJ mol^{-1} and 108 kJ mol^{-1}, respectively) differ by 16 kJ mol^{-1}. Assuming first-order kinetics with an excess of empty cages **1a** and **2a** in the ^{1}H NMR experiments, this energy difference translates to a factor of about 230 between the two reaction rate constants at 80 °C. Thus, cage **1a** incorporates water 230 times faster than cage **2a**, whose orifice is blocked by the stopper group. This result concurs with the observations in the ^{1}H NMR experiments. From the encapsulation ratio of approximately 100:1 found in the experiments for cage **1a** and **2a**, a difference in barrier heights of about 13 kJ mol^{-1} can be estimated that compares well to the computed value of 16 kJ mol^{-1}.

In summary, by chemical transformation of an intact [60]fullerene cage, an open-cage fullerene was synthesized that works perfectly as a lockable molecular container for a single water molecule. A reversibly bound phosphate moiety located above the orifice acts as an effective stopper to block the opening of the cage and thus trap the encapsulated water molecule. ^{1}H NMR experiments and theoretical investigations show that with the stopper attached the reaction rates for the encapsulation and release process of the water molecule are drastically reduced relative to the unblocked open cage. Thus, the reported system represents a molecular vial that can be opened and closed in an easy single step reaction, suggesting possible applications as a transporter or carrier.

Experimental Section

Compound **2a**: $P(OEt)_3$ (50 mg, 0.27 mmol) was slowly added to a solution of compound **1a** (33 mg, 0.033 mmol) in toluene (10 mL) at 20 °C. The progress of the reaction was monitored by TLC. The reaction was stopped when **2a** reached its maximum yield (ca. 10 min). The solution was directly chromatographed on a silica gel column eluting with toluene/acetic ether (100:1). The first red band was a trace amount of unreacted starting material **1a.** The second red band was collected and evaporated to give **2a** as an orange solid (24 mg, 0.021 mmol, 64 %). Characterization data: ^{1}H NMR ([D_4]-*ortho*-dichlorobenzene (ODCB), 600 MHz): δ = 7.87 (d, 4H), 7.62 (s, 2H), 7.37 (d, 1H), 7.20 (t, 4H), 6.90 (d, 2H), 4.58–4.45 (4H), 1.33 ppm (t, 6H). ^{13}C NMR ([D_4]-ODCB, 150 MHz): All signals represent 2C except where otherwise noted. δ = 185.33, 174.09 (1C), 154.77, 149.76, 149.03, 148.89, 148.82, 148.46, 148.21 148.03, 147.79, 147.43, 147.33, 147.22, 146.62, 146.06, 145.29, 144.73, 143.69, 143.17, 142.97, 142.86, 142.77, 142.40, 141.64, 140.61, 139.58, 133.85, 132.91, 132.57, 130.67, 128.85(4C), 127.95 (4C), 123.79, 80.86 77.70, 77.31, 64.35, 16.33 ppm. FTIR (microscope): 3251, 2966, 2920, 1738, 1463, 1378, 1283, 1097, 1031, 964, 769, 695 cm^{-1}. ESI-HRMS (for $C_{76}H_{24}N_2O_9P$ [M+H$^+$]: calculated 1139.1214, found 1139.1269.

Crystal data for **2a**: crystal size, 0.20 × 0.20 × 0.15 mm^3, triclinic, space group $P\bar{1}$, a = 12.372(3), b = 13.972(3), c = 14.496(3) Å, α = 74.66(3), β = 83.10(3), γ = 76.24(3)°, V = 2342.8(8) Å^3, Z = 2, ρ_{calcd} = 1.619 Mg m^{-3}; T = 173(2) K; 28960 reflections collected, 10661 independent (R_{int} = 0.0360) included in the refinement; min/max transmission = 0.9793 and 0.9726; refinement method full-matrix least-squares on F^2. Final R indices [$I > 2\sigma(I)$] $R1$ = 0.0525, $wR2$ = 0.1392, R indices (all data) $R1$ = 0.0564, $wR2$ = 0.1428. One of the methyl groups is disordered over two orientations.

CCDC 783509 contains the supplementary crystallographic data for this paper. These data can be obtained free of charge from The Cambridge Crystallographic Data Centre via www.ccdc.cam.ac.uk/data_request/cif.

Hydrolysis of **2a**: KOH (5 mL, 0.1M) was added to a solution of **2a** (12 mg, 0.011 mmol) in CH_2Cl_2 (15 mL) at room temperature. After stirring for several minutes, [18]crown-6 (6 mg) was added to the solution. Progress of the reaction was monitored by TLC. The reaction was stopped when **1a** reached its maximum yield (ca. 2 h). The solution was washed with water (20 mL × 3). The organic layer was separated and directly chromatographed on silica gel eluting with toluene/acetic ether (100:1). The first red band was collected and evaporated to give **1a** as an orange solid (3 mg, 0.003 mmol, 27 %).

Density functional theory: DFT calculations including an empirical correction term for dispersion (DFT-D) were conducted for the empty cages **1a**, **2a**, and their water-encapsulation complexes H_2O@**1a** and H_2O@**2a** with the program package TURBOMOLE using the resolution of the identity (RI) approximation.[9] Based on our previous successful benchmark and computational studies for carbon nanotubes and fullerenone cages, the DFT-D parameterisation of Grimme from 2004 along with the BP86 functional was employed.[8] The equilibrium structures were optimized in the def2-TZVP basis set, but for the determination of the reaction barriers, both the equilibrium and the transition state structures were optimized using the smaller def2-SV(P) basis set. The final binding energies and barriers were subsequently calculated as single points with the large def2-TZVP basis set.[10] All energies are corrected for the basis set superposition error (BSSE).[11] To create best-guess starting structures for the subsequent transition state search calculations, perpendicular

scans for water leaving the cage were performed for H_2O@**1a** and H_2O@**2a**. Starting from the equilibrium position within the cage, the water molecule was moved towards the orifice along the OX direction in steps of 0.5 Å (X is the center of the bottom pentagon in the cage, opposite to the opening). For each structure along these pathways, the perpendicular position of the water molecule was fixed by freezing the distance, angle, and dihedral angle of the oxygen atom with respect to the bottom pentagon while optimizing all other degrees of freedom (BP86-D/def2-TZVP). The scans were refined by reducing the step size to 0.1–0.2 Å within the maximum energy region. The maximum energy structures within these scans were then used for the final saddle point searches employing the surface walking algorithm of the module STATPT. Several restarts with a recomputed exact hessian were needed to finally locate the saddle points.[12] A true TS (one imaginary frequency) was found for H_2O@**2a**, whereas the adopted TS structure for H_2O@**1a** revealed two imaginary frequencies with respect to not only the reaction coordinate but also an energetically almost irrelevant rotation of the water molecule. To estimate the influence of the solvent on the binding energies and barrier heights, the perpendicular scans for H_2O@**1a** and H_2O@**2a** were repeated with a continuum solvation model, the conductor-like screening model (COSMO, $\varepsilon = \infty$).

Received: August 5, 2010
Published online: November 16, 2010

Keywords: density functional calculations · fullerenes · molecular devices · supramolecular chemistry

[1] a) Y. Rubin, *Top. Curr. Chem.* **1999**, *199*, 67; b) J.-F. Nierengarten, *Angew. Chem.* **2001**, *113*, 3061; *Angew. Chem. Int. Ed.* **2001**, *40*, 2973; c) M. Murata, Y. Murata, K. Komatsu, *Chem. Commun.* **2008**, 6083; d) G. C. Vougioukalakis, M. M. Roubelakis, M. Orfanopoulos, *Chem. Soc. Rev.* **2010**, *39*, 817; e) L. B. Gan, D. Z. Yang, Q. Y. Zhang, H. Huang, *Adv. Mater.* **2010**, *22*, 1498.

[2] a) J. C. Hummelen, M. Prato, F. Wudl, *J. Am. Chem. Soc.* **1995**, *117*, 7003; b) G. Schick, T. Jarrosson, Y. Rubin, *Angew. Chem.* **1999**, *111*, 2508; *Angew. Chem. Int. Ed.* **1999**, *38*, 2360; c) K. Komatsu, M. Murata, Y. Murata, *Science* **2005**, *307*, 238; d) M. Murata, Y. Murata, K. Komatsu, *J. Am. Chem. Soc.* **2006**, *128*, 8024; e) S.-i. Iwamatsu, T. Uozaki, K. Kobayashi, S. Y. Re, S. Nagase, S. Murata, *J. Am. Chem. Soc.* **2004**, *126*, 2668; f) Z. Xiao, J. Y. Yao, D. Z. Yang, F. D. Wang, S. H. Huang, L. B. Gan, Z. S. Jia, Z. P. Jiang, X. B. Yang, B. Zheng, G. Yuan, S. W. Zhang, Z. M. Wang, *J. Am. Chem. Soc.* **2007**, *129*, 16149; g) H. Hachiya, Y. Kabe, *Chem. Lett.* **2009**, *38*, 372; h) Q. Y. Zhang, Z. S. Jia, S. M. Liu, G. Zhang, Z. Xiao, D. Z. Yang, L. B. Gan, Z. M. Wang, Y. L. Li, *Org. Lett.* **2009**, *11*, 2772.

[3] a) Y. Rubin, T. Jarrosson, G. W. Wang, M. D. Bartberger, K. N. Houk, G. Schick, M. Saunders, R. J. Cross, *Angew. Chem.* **2001**, *113*, 1591; *Angew. Chem. Int. Ed.* **2001**, *40*, 1543; b) C. M. Stanisky, R. J. Cross, M. Saunders, M. Murata, Y. Murata, K. Komatsu, *J. Am. Chem. Soc.* **2005**, *127*, 299; c) Ref. [2e]; d) K. E. Whitener, Jr., R. J. Cross, M. Saunders, S.-i. Iwamatsu, S. Murata, N. Mizorogi, S. Nagase, *J. Am. Chem. Soc.* **2009**, *131*, 6338; e) Y. Morinaka, F. Tanabe, M. Murata, Y. Murata, K. Komatsu, *Chem. Commun.* **2010**, *46*, 4532.

[4] Ref. [2h].

[5] R. Engel, *Org. React.* **1988**, *36*, 175; for a recent example; see: P. G. Mandhane, R. S. Joshi, D. R. Nagargoje, C. H. Gill, *Tetrahedron Lett.* **2010**, *51*, 1490.

[6] L. El Kaïm, L. Gaultier, L. Grimaud, A. D. Santos, *Synlett* **2005**, 2335.

[7] S.-C. Chuang, Y. Murata, M. Murata, K. Komatsu, *Chem. Commun.* **2007**, 1751.

[8] a) T. Pankewitz, W. Klopper, *Chem. Phys. Lett.* **2008**, *465*, 48; b) T. Pankewitz, W. Klopper, *J. Phys. Chem. C* **2007**, *111*, 18917; c) S. Grimme, *J. Comput. Chem.* **2004**, *25*, 1463.

[9] a) TURBOMOLE V6.1 V6.2 **2009–2010**, a development of University of Karlsruhe (TH) and Forschungszentrum Karlsruhe GmbH, 1989–2007, TURBOMOLE GmbH since 2007; http://www.turbomole.com; b) R. Ahlrichs, M. Bär, M. Häser, H. Horn, C. Kölmel, *Chem. Phys. Lett.* **1989**, *162*, 165; c) O. Treutler, R. Ahlrichs, *J. Chem. Phys.* **1995**, *102*, 346; d) R. Ahlrichs, *Phys. Chem. Chem. Phys.* **2004**, *6*, 5119.

[10] a) A. Schäfer, H. Horn, R. Ahlrichs, *J. Chem. Phys.* **1992**, *97*, 2571; b) F. Weigend, M. Häser, H. Patzelt, R. Ahlrichs, *Chem. Phys. Lett.* **1998**, *294*, 143; c) F. Weigend, R. Ahlrichs, *Phys. Chem. Chem. Phys.* **2005**, *7*, 3297; d) F. Weigend, *Phys. Chem. Chem. Phys.* **2006**, *8*, 1057.

[11] S. F. Boys, F. Bernardi, *Mol. Phys.* **1970**, *19*, 553.

[12] a) P. Deglmann, F. Furche, R. Ahlrichs, *Chem. Phys. Lett.* **2002**, *362*, 511; b) P. Deglmann, F. Furche, *J. Chem. Phys.* **2002**, *117*, 9535; c) P. Deglmann, K. May, F. Furche, R. Ahlrichs, *Chem. Phys. Lett.* **2004**, *384*, 103.

